



## SEISMIC STRENGTH MODELS FOR BEAM-COLUMN JOINTS IN EXISTING CONCRETE BUILDINGS

### Wael M. Hassan

Assistant Professor of Structural Engineering, American University in Cairo, New Cairo, Egypt  
*waelhassan@aucegypt.edu*

### Jack P. Moehle

T.Y. and Margaret Lin Professor of Engineering, University of California, Berkeley, USA  
*moehle@berkeley.edu*

**ABSTRACT:** Earthquake reconnaissance has reported the substantial damage that can result from inadequate concrete beam-column joints in earthquake shaking. In some cases, failure of older-type corner joints appears to have led to building collapse. Since the 1960s, many advances have been made to improve seismic performance of building components, including beam-column joints. New design and detailing approaches are expected to produce new construction that will perform satisfactorily during strong earthquake shaking. Much less attention has been focused on joints of older construction, lacking transverse reinforcement, that may be seismically vulnerable. The available literature concerning the performance of such joints is relatively limited, but concerns about performance exist. The goal of this paper is to provide mathematical assessment tools for seismic strength of unconfined exterior and corner joints in existing buildings. In particular, it aims to quantify shear strength, bond pullout strength and residual axial capacity of seismically shear damaged joints. Five seismic strength models are developed and presented in this paper. A strut-and-tie model along with a simplified empirical model for shear strength evaluation are presented. In addition, a bond capacity model is introduced to assess the pullout strength of the short-embedded beam reinforcement in joints, a typical detail in many existing buildings. Moreover, two joint axial capacity models, designed specifically for unconfined joints based on the shear friction concept, are presented. All proposed models correlated well with previous test results.

### 1. Introduction

Beam-column joints in concrete buildings are key components to ensure structural integrity of building performance under seismic loading. Earthquake reconnaissance has shown the substantial vulnerability and structural damage that can result from inadequacy of beam-column joints. In some cases, failure of older-type corner joints appears to have led to building collapse (Figs. 1 and 2). Since the 1960s, tremendous research efforts have been devoted to develop tools to fulfill adequate seismic performance of components of concrete structures, including beam-column joints. These efforts included developing new design concepts along with new ductile details to provide sufficient deformability and satisfactory performance during earthquake excitations.

However, much less research attention has been paid to understanding the performance of existing substandard buildings not designed as seismically resistant, although they constitute the vast majority of building inventory in many countries. Concrete buildings constructed prior to developing ductile details in the 1970s normally lack joint transverse reinforcement. The available literature concerning the performance of beam-column joints without transverse reinforcement, denoted “unconfined” joints in this paper, is relatively limited. Most researchers focused on testing and modeling unconfined interior and exterior beam-column joints. There is very scarce available published test data concerning the seismic performance of unconfined corner beam-column joints. The literature body lacks joint shear strength

models designed particularly for unconfined joints. In addition, the axial capacity and potential to axial failure of unconfined beam-column joints is still highly unknown. No mathematical models exist to assess residual axial capacity of beam-column joints following joint shear failure, which reflects the potential of building total or partial collapse. This paper presents some proposed mathematical tools to assess the seismic shear strength, bond strength and residual axial capacity of exterior and corner unconfined joints.

Hassan (2011) identified the modes of failure of unconfined beam-column joints under seismic load reversals. The primary failure mode is J-Failure, or the direct joint shear failure without beam or column yielding or pullout failure of beam bars. The BJ-Failure and CJ-Failure modes represent joint shear failure following beam or column yielding, respectively. S-Failure mode represents the bottom beam bar short embedment pullout bond-slip failure. Hassan (2011) hypothesizes that the "true" joint shear capacity is the one corresponding to J-Failure mode. The other three failure modes' strengths are trivial as they correspond to the yielding or bond capacities of the members framing into the joint, which represent capping strength values that jeopardize joint strength if they were reached prior to reaching the "true" direct joint shear strength of J-Failure mode.



**Fig. 1 – Structure Collapse due to Failure of Deficient Beam-column Joints, Kaiser Permanente Building, Northridge Earthquake, 1994 (Photo Credit, G. Edstrom)**



**Fig. 2 – Joint Failure and Partial Building Collapse in the March 13, 1992, Erzincan, Turkey Earthquake, (Photo Credit, Zahertar)**

## 2. Joint Shear Strength Models

### 2.1. Modified J-Failure Strut-and-Tie Model.

The major problem encountered when applying strain-based strut-and-tie models (STM) to unconfined beam-column joints is the uncertainty in the expressions for computing principal tensile strains as they are strongly affected by crack width from early loading stages. This problem is more pronounced in plain concrete in unconfined joints. Crack width is not a practical quantity to use in design and hence it was not reported in most past tests. It was then decided in this study not to rely on explicit expressions for tensile strains or crack width in estimating softening of the concrete strut in developing shear strength models for unconfined joints. Instead, a global softening coefficient value based on regression analysis of previous joint test results was sought. The shortcomings of the available STMs in shear strength prediction of J-Failure modes motivated the search for a simpler model that accommodates the force transfer mechanism in unconfined exterior joints. The controversial assessment of softening strut coefficient based on principal strains led to revisiting the simple concept of a direct strut that incorporates a softening coefficient suitable for each individual case, namely the ACI 318-11 STM approach. Figure 3 depicts the proposed model.

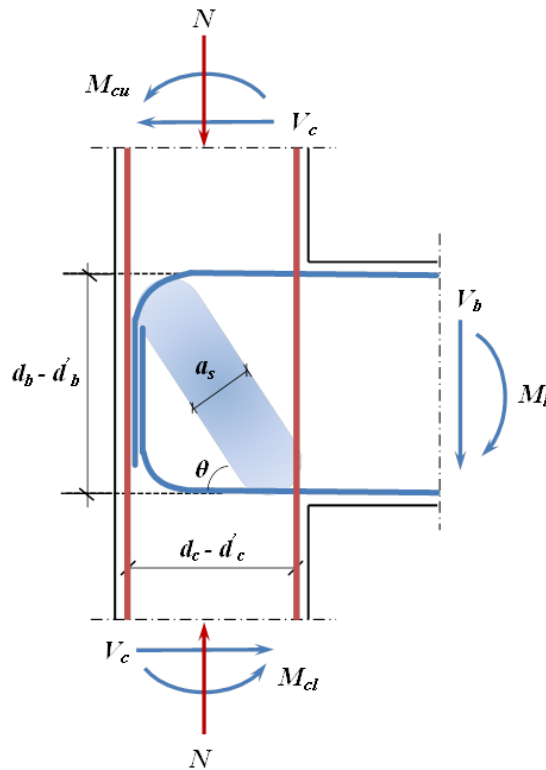


**Fig. 3 – Proposed Strut-and-tie Model**

The effective strut compressive strength  $f_{cu}$  and diagonal strut capacity  $D$  are

$$f_{cu} = 0.85\beta_s f'_c \quad (1)$$

$$D = f_{cu} A_{str} \quad (2)$$

where  $\beta_s$  is concrete softening coefficient. According to ACI 318-11, for the case of a bottle-shaped strut with no crack control reinforcement,  $\beta_s = 0.6$ .  $A_{str}$  is the concrete strut area calculated by

$$A_{str} = a_s b_j \quad (3)$$

where  $b_j$  is the effective joint width defined by ACI 352R-02 and  $a_s$  is the strut depth defined as

$$a_s = \sqrt{a_b^2 + a_c^2} \quad (4)$$

$a_b$  and  $a_c$  are the compression zone depths of the beam and column, respectively.  $a_b$  can be estimated by locating the neutral axis of transformed cracked linear beam section:

$$a_b = kd_b \quad (5)$$

$$k = [(\rho + \rho')^2 n^2 + 2(\rho + \rho' \frac{d_b'}{d_b})n]^{1/2} - (\rho + \rho')n \quad (6)$$

where  $d_b$  and  $d_b'$  are depths from extreme compression fiber to centroids of beam tension and compression longitudinal reinforcement, respectively,  $n$  is the modular ratio, and  $\rho$  and  $\rho'$  are beam tension and compression reinforcement ratios, respectively. The quantity  $a_c$  can be estimated by:

$$a_c = (0.25 + 0.85 \frac{P}{f_c' A_g}) h_c \leq 0.4h_c \quad (7)$$

where  $P$  is column axial load and  $A_g$  is gross section area. The above calculation of  $a_b$  and  $a_c$  is based on the assumption that neither the beam nor the column is not yielding before the joint reaches the shear capacity in J-Failure mode. The expression for  $a_c$  accommodates the effect of column axial load on joint shear strength. Past tests indicate that increasing axial load can result in a 10% -20% increase in shear strength, (Hassan and Moehle, 2012). The limit on  $a_c = 0.4h_c$  is proposed so that the calculated strength increase due to axial load is limited accordingly.

The choice of a softening coefficient  $\beta_s$  of 0.6 for a bottle-shaped strut with no crack control reinforcement is an interpretation of ACI 318-11 code provisions for unconfined joints. Accordingly, joint shear strength based on diagonal strut capacity without including the effect of intermediate column reinforcement is:

$$V_j = D \cos \theta \quad (8)$$

$$\theta = \tan^{-1} \left( \frac{d_b - d_b'}{d_c - d_c'} \right) \quad (9)$$

where  $d_c$  and  $d_c'$  are depths from extreme compression fiber to centroids of tension and compression longitudinal reinforcement in the column, respectively. The joint shear strength coefficient for joints experiencing J-Failure mode is:

$$\gamma_j = \frac{V_j}{h_c b_j \sqrt{f_c'}} \quad (10)$$

It is noteworthy to mention that the model adopts the hydrostatic node assumption, whereby equal pressure is sustained by the three edges of the node and, hence, the strut strength controls the failure. The shear strength calculated from Eq. 10 is for a unidirectional loading within the plane of the frame. Therefore, this shear strength expression is applicable to exterior joints or corner joints under unidirectional loading. For a corner joint undergoing bidirectional framing, an elliptical biaxial shear strength interaction is suggested (Hassan 2011)

## 2.2. J-Failure Empirical Shear Strength Model.

In Hassan (2011), the effects of the major parameters influencing joint shear strength were presented. This enabled establishing empirical expressions for the effect of the most important parameters on shear strength of J-Failure mode joints, namely joint aspect ratio and axial load ratio. The empirical factors were derived first for each individual parameter based on the observed trend of the effect of the parameters considered on joint shear strength. Consequently, an empirical shear strength expression (Eq. 11) was

developed to take into account collectively the effects of both axial load ratio and joint aspect ratio. The empirical constant was used to adjust the overall shear strength expression to best fit the trend of model-to-test shear strength. This empirical model can serve as a preliminary means for quick estimation of joint shear strength with sufficient accuracy, without the need to perform strut capacity calculations. The empirical joint shear strength expression is given by:

$$V_j = 11\alpha_j^{-0.50}\kappa b_j h_c \sqrt{f'_c} \quad (11)$$

where the joint aspect ratio  $\alpha_j$  is:

$$\alpha_j = \frac{h_b}{h_c} \quad (12)$$

The effect of axial load is reflected through the factor  $\kappa$ . A linear interpolation is suggested to obtain the axial load factor  $\kappa$  between the two boundary aspect ratios  $\alpha_j=1$  and  $\alpha_j=2$ .

$$\kappa = 1 + (0.86 - 0.31\alpha_j) \left[ \frac{P}{f'_c A_g} - 0.15 \right] \quad \text{where} \quad 1 \leq \kappa \leq 1.2 \quad (13)$$

Finally, the shear strength coefficient is calculated:

$$\gamma_j = \frac{V_j}{h_c b_j \sqrt{f'_c}} \quad (14)$$

### 2.3. BJ-Failure Shear Strength Model.

Previous tests on unconfined beam-column joints experiencing beam yielding before joint shear failure, (Hassan and Moehle 2012), suggest an inherent relationship between joint shear strength and the flexural capacity of yielding beam. Specifically, the flexural resistance of a yielding beam decides the limiting joint shear demands and, as yielding progresses, joint strength degrades until joint shear failure occurs, usually shortly after onset of beam yielding. Hence, the joint shear strength is the shear corresponding to development of beam flexural strength. In some tests, there is some minor joint shear strength gain after flexural beam yielding. This is attributed to strain hardening of beam reinforcement. Since the strength overshoot is slight and uncertain, it is recommended to limit joint shear strength to the joint shear corresponding to beam flexural yielding strength.

### 2.4. Shear Strength Models Evaluation.

A database of 29 exterior and corner joint tests were used to test the accuracy of shear strength prediction of the proposed modified ACI 318-11 strut-and-tie model for joints experiencing J-failure mode. The details of database are presented elsewhere, (Hassan, 2011). Figure 4 displays the correlation between test joint shear strength coefficients and those calculated by the proposed modified ACI 318-11 STM model for J-Failure joints. The accuracy of the model is reflected in the average test to model shear strength ratio of 1.03 with coefficient of variation of 0.11. The average dispersion coefficient is 0.02 ranging from 0.01 to 0.05. The figure shows the mean plus and minus standard deviation range.

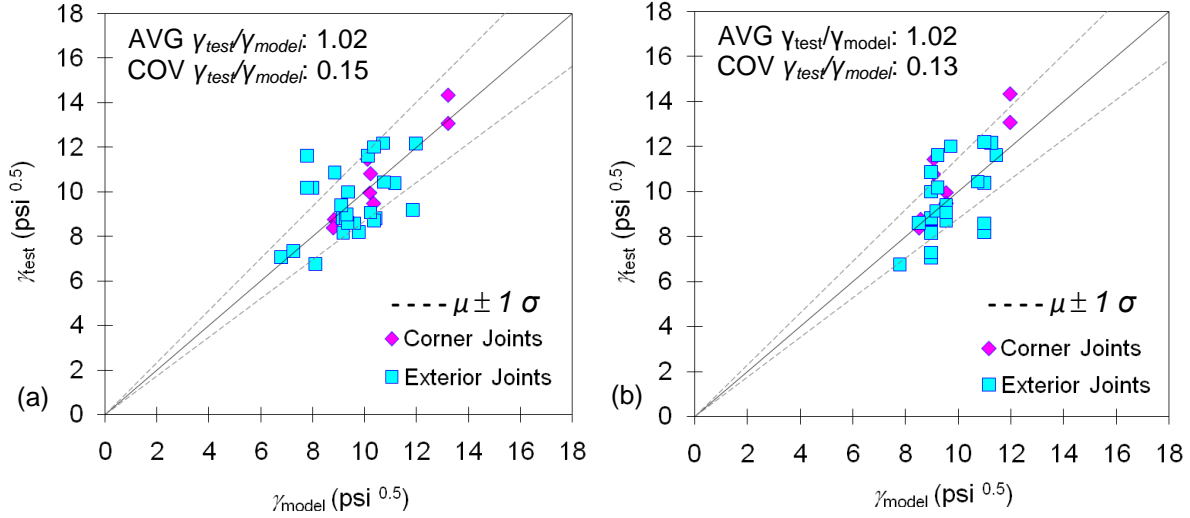


**Fig. 4 – Experimental Verification of Proposed a) STM Model, b) Empirical Shear Strength Model**

Figure 4 displays also the correlation of test results to joint shear strength calculated using the proposed empirical shear strength expression Eq. 11. Average test-to-model joint shear strength coefficient is 0.99 while the COV is 0.13. This reveals the accuracy of the proposed empirical expression for quick estimation of unconfined exterior and corner joint shear strength for preliminary assessment purposes.

### 3. Joint Bond Strength Model

The present study was motivated to explore whether improvements could be achieved in empirical equations to estimate the bond strength of short embedded bars (Fig. 5) by including influential parameters such as axial load, beam bar diameter, cover to bar diameter ratio, and presence of transverse beams orthogonal to joint. The following expression was developed to represent the concrete average bond stress capacity of beam bottom reinforcement with insufficient embedded length:

$$\tau_{\max} = 13.2 \left( \frac{P}{f_c' A_g} \right)^{0.25} \sqrt{f_c'} \Psi_s \Omega \left( \frac{c}{d} \right) \geq 6 \sqrt{f_c'} \quad (15)$$

where  $P$  is column axial load,  $\Psi_s$  is bar diameter factor, and  $\Omega$  is transverse beam confinement factor, defined as follows:  $\Psi_s = 1$  for bar diameter  $\geq 0.75$  in. and 1.25 for bar diameter  $< 0.75$  in.,  $\Omega = 1$  for exterior isolated joints, 1.12 for joints with transverse beam on one side, and 1.20 for joints with transverse beam on both sides.  $(c/d)$  is the minimum of bottom and side concrete cover-to-bar diameter ratio measuring cover to bar centroid, which is not to exceed 2.5. The power term in the above expression is intended to account for axial load level and is calibrated from test results of the S-Failure database assembled in Hassan (2011). For consistency with the presentation method of the current paper and for comparison to other failure modes, this model is presented in terms of joint shear stress coefficient  $\gamma_{sj}$ , corresponding to pullout failure, although joint shear strength in this case is not fully engaged. In all tests of the database used, pullout failure occurred before bar yielding. Thus, Eq. 17 is only applicable for this case with no bar yielding, which is very likely in bond-slip failure of short embedded bar. However, it is recommended to develop a future extension of this expression to cases with bar yield for more generality. A database of twenty-five previous exterior and corner joint tests was used to test the accuracy of the proposed empirical bond strength model for joints experiencing pullout S-failure mode. The details of these tests were presented in Hassan (2011).

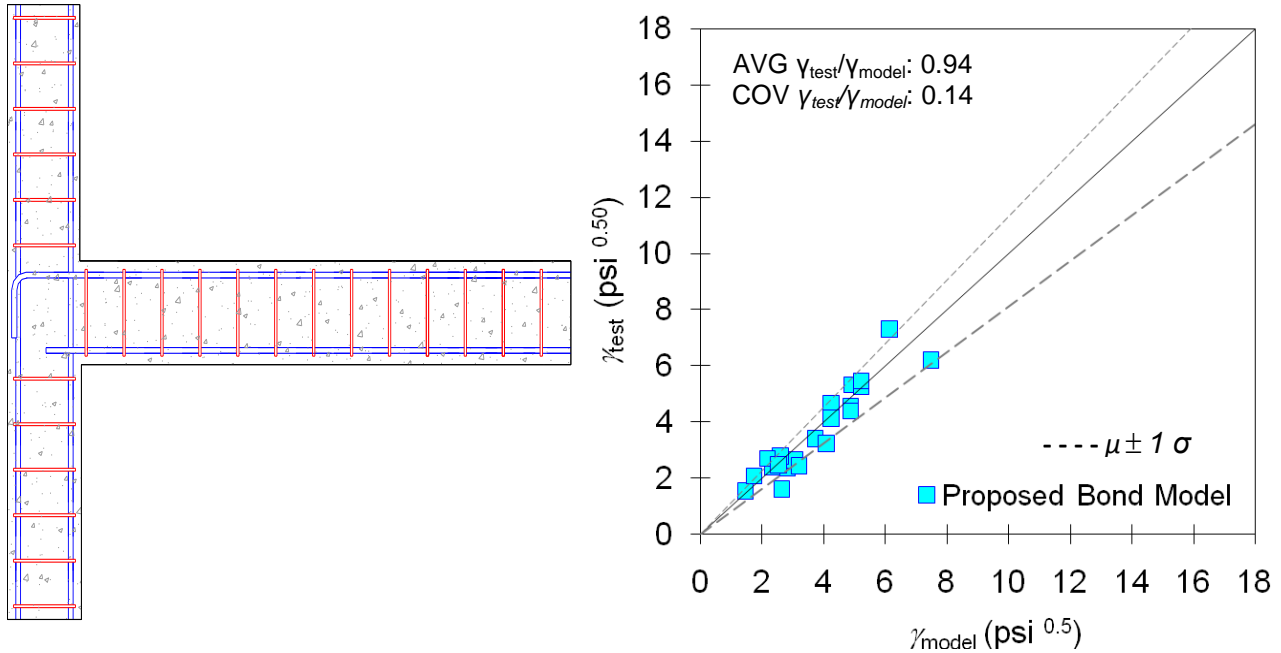


**Fig. 5 – Experimental Verification of Proposed S-Failure Bond Strength Model**

Figure 5 exhibits joint shear stress coefficient corresponding to experimental and calculated empirical model bond capacities. Correlation parameters reflect 0.94 mean test-to-model strength ratio associated with a 0.14 coefficient of variation. These values indicate the relative accuracy of the proposed empirical bond model. More tests would be useful to further verify and refine this empirical model.

## 4. Joint Axial Capacity Model

### 4.1. Theoretical Basis

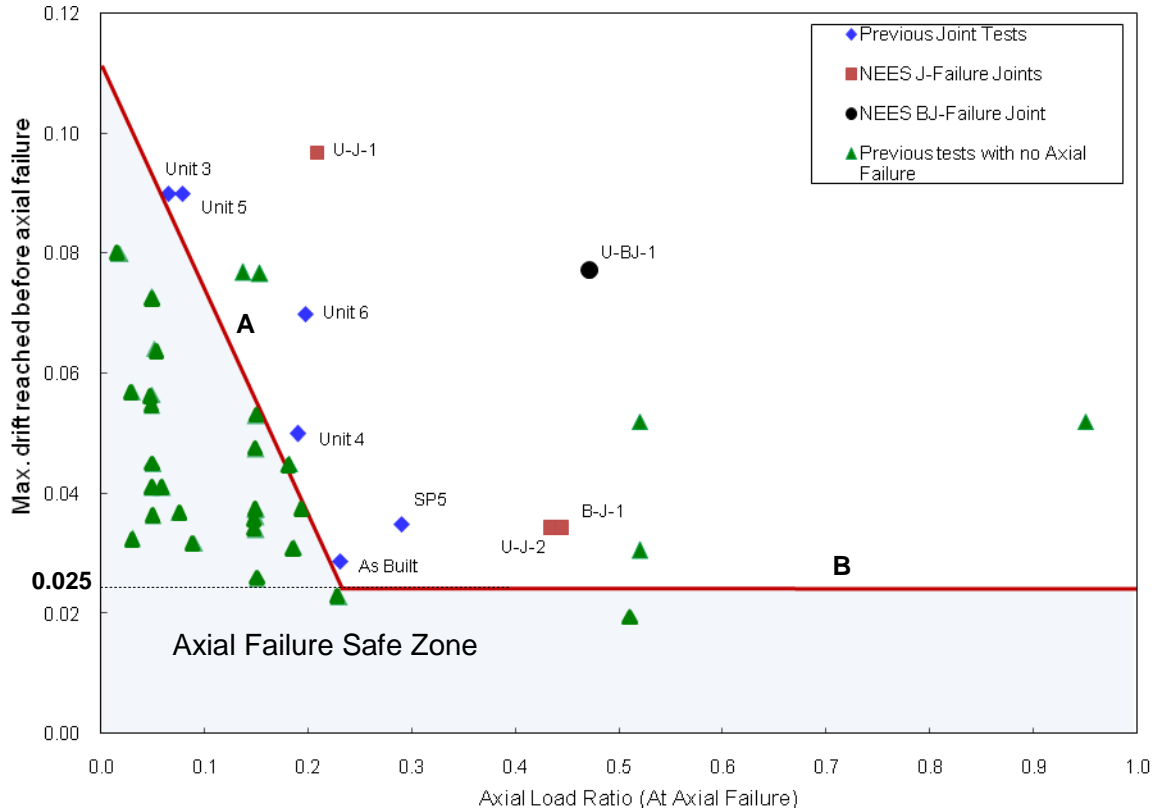
Axial failure of unconfined joints is evident during many past earthquakes, (Hassan and Moehle 2013). No analytical models exist to predict the residual joint axial capacity following seismic shear failure. Unfortunately, only few previous joint tests were continued until reaching axial failure.

Figure 6 plots the relationship between axial failure load and the maximum drift reached prior to axial failure for a database of 47 previous exterior and corner joint tests, of which axial failure was reached in only 10 tests (Hassan 2011). The axial load ratio and drift ratio for this database reflect the test termination values. The size of axial failure joints database is relatively small compared to that of non-axial failure joints. However, several useful observations can be made from this plot. It appears that exterior and corner joints may be susceptible to axial failure under very large drifts or under high axial loads. A general trend of a decreased axial failure drift capacity for J-Failure mode is associated with higher axial loads. Based on previous joint tests that did not experience axial failure, an axial failure safe zone can be drawn as shown in Fig. 6. Inclined line *A* defines a fairly clear demarcation between tests with and without axial failure. Line *B* (drifts ratios below 2.5%) is more tenuous, as it extends to high axial load levels for which few tests are available. The inclined line *A* can be algebraically expressed as

$$\left(\frac{\Delta}{L}\right) \leq \frac{1}{9} - \frac{P}{2.72 f_c' A_g} \quad (16)$$

Based on Elwood and Moehle (2003) axial capacity model for columns, an analogous model for application to unconfined joints is proposed. The model is based on observation of axial failure modes. The model assumes that the primary failure mechanism is along a shear friction surface of the previously

shear-damaged joint (Fig. 7), with column longitudinal reinforcement acting in axial load providing a secondary mechanism triggered after shear-friction failure on the shear failure plane. This section presents two axial capacity models for unconfined beam-column joints. These models are intended to be used with joints experiencing J-shear failure mode with any axial load level and BJ-failure mode with axial load ratio below 0.3. As discussed in Hassan (2011), the axial failure of a BJ shear failure controlled joint under high axial load is not likely until very large drifts.



**Fig. 6 – Axial Load-Drift Ratio Relationship at Axial Failure (or Test Termination) for Exterior and Corner Joints, (Hassan and Moehle, 2013)**

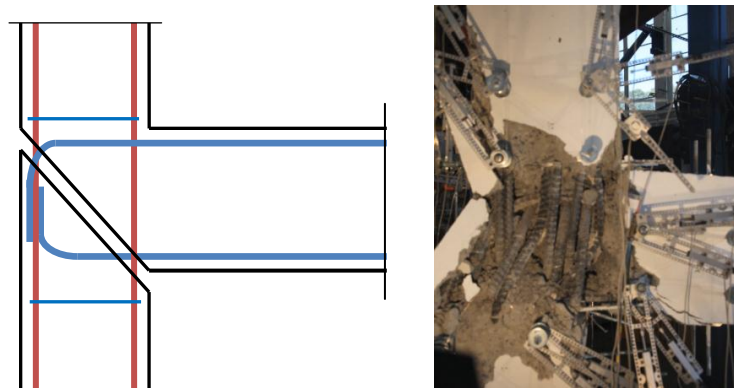


**Fig. 7 – Development of Shear-friction Model for Joint Axial Capacity Based on Experimental Observation, (a) Proposed Sliding Mechanism, (b) Damage after Axial Failure, (Hassan 2011)**

## 4.2. Analytical Shear-Friction Capacity Model

After joint shear failure along the major diagonal crack corresponding to the inclination of the main diagonal concrete joint strut, shear resistance starts to degrade. In many cases, however, the axial load at peak displacement does not immediately drop as discussed Hassan and Moehle (2012). Substantial axial load from the upper column must be transferred across the joint shear failure surface. Experimental observation of joint axial failure suggests transferring this axial load by shear-friction across the shear failure plane. Several shear-friction models are available; however, the classical shear-friction model adopted by ACI 318-11 and used by Elwood and Moehle (2003) for shear-critical columns is used here.

Figure 8 shows the free body diagram of the upper block of the beam-column joint sub assemblage after shear failure. The critical crack angle  $\theta$  can be calculated using the strut-and-tie model developed in Hassan (2011) for joint shear strength. The axial failure is evident to take place during the downward loading of beam. Some simplifying assumptions are made next.

$V_b$  and  $V_j$  are the beam shear force and joint shear force at joint shear failure, respectively. Since the beam shear force  $V_{b,a}$  and joint shear force  $V_{j,a}$  at axial failure are not always insignificant like the case of columns (Elwood and Moehle 2003), they cannot be neglected in formulating the equilibrium equations. The dowel action provided by the longitudinal column and beam reinforcement will be implicitly included in the shear friction resistance  $V_{sf}$ ; hence they will not appear in the equilibrium equations. The total axial capacity of column reinforcement bars is denoted  $\Sigma P_s$ . The beam longitudinal reinforcement will act as shear-friction reinforcement holding the lower concrete block (the column) from separation. At the axial failure, the force in both top and bottom longitudinal beam bars will be tensile within the joint regardless the sense of the force within beam span.

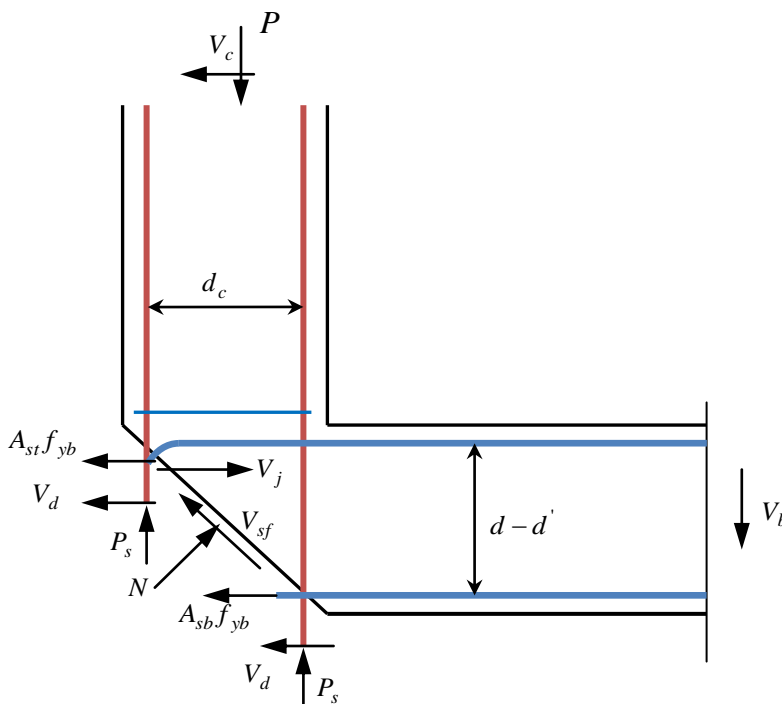


**Fig. 8 – Free Body Diagram for Beam-Column Joint at the Onset of Axial Failure**

The top beam longitudinal reinforcement appears to be less efficient in resisting shear friction since it experiences bond failure at earlier stage. More importantly, the portion of the top beam bars holding the lower concrete block is usually the hook tail which is very poorly embedded and bonded to concrete at late stages of loading because of cover spalling or detachment. Accordingly, the resistance of top beam bars will not be included in the equilibrium equations. Based on the abovementioned simplifying

assumptions, the equilibrium equations in the horizontal and vertical directions can be respectively written as:

$$N \sin \theta + V_j = V_{sf} \cos \theta + A_{sb} f_{yb} + \Sigma V_d \quad (17)$$

$$P + V_b = N \cos \theta + V_{sf} \sin \theta + \Sigma P_s \quad (18)$$

The proposed model assumes that joint axial capacity is primarily dependent on shear-friction mechanism. Column longitudinal axial capacity is considered secondary to shear-friction mechanism, which is triggered only after shear-friction failure. The calculation of axial capacity of column bars presented in Hassan (2011), shows that this capacity is relatively small. Even if a portion of axial load is supported by column bars immediately before axial failure, suggesting a concurrent collective mechanism, this portion is insignificant as suggested by Elwood and Moehle (2003). Accordingly, this quantity will not be included in the model. Only the final model equations are presented herein for brevity. The model derivation is thoroughly presented in Hassan (2011). The model relates the axial load  $P$  to the drift capacity at axial failure  $(\Delta/L)_{axial}$ . It can also be used reversely to find the axial load capacity for a given drift ratio. More test data regarding axial failure of exterior and corner beam column joints is needed to refine and validate the expressions for lateral load capacity at axial failure.

$$\left( \frac{\Delta}{L} \right)_{axial} = 0.03 \left\{ \frac{(P + V_{b,a}) \tan \theta + (V_{j,a} - A_{sb} f_{yb})}{(P + V_{b,a}) - (V_{j,a} - A_{sb} f_{yb}) \tan \theta} \right\}^{-0.25} \quad (19)$$

$$\left( \frac{\Delta}{L} \right)_{axial} = 0.03 \left\{ \frac{(P + \chi \chi_a V_j) \tan \theta + (\chi_a V_j - A_{sb} f_{yb})}{(P + \chi \chi_a V_j) - (\chi_a V_j - A_{sb} f_{yb}) \tan \theta} \right\}^{-0.25} \quad (20)$$

$$V_{j,a} = \left( 1.1 \frac{P}{f_c' A_j} - 0.03 \right) V_j = \chi_a V_j \quad (21)$$

$$V_{b,a} = \left( 1.1 \frac{P}{f_c' A_j} - 0.03 \right) V_b = \chi_a V_b \quad (22)$$

$$V_b = \frac{1}{\frac{L - h_c/2}{jd_b} - \frac{L}{H}} = \chi V_j \quad (23)$$

where:  $L$  is half the beam span,  $H$  is floor height,  $h_c$  is column depth,  $j=0.9$ , and  $d_b$  is the effective beam depth.

### 4.3. Empirical Shear-Friction Axial Capacity Model

The above theoretically based shear-friction model is plausible if enough knowledge on the residual joint shear capacity at axial failure can be confirmed. It also contains two empirical components, namely the estimation of effective shear-friction coefficient and the residual shear capacity at axial failure. The model is delivered finally in a rather lengthy expression. These factors motivated investigating the possibility of the presence of a trend between drift ratio and the axial failure load normalized by the influential parameters of the shear-friction phenomenon. The goal of this attempt was to develop a simpler empirical expression for quick estimation of drift capacity at axial failure eliminating the need for residual joint shear strength at axial failure. An empirical expression can be developed based on shear friction influence parameters. Figure 9 shows the relationship between drift ratio at axial failure and the axial failure load normalized by beam bottom reinforcement strength (acting as shear friction reinforcement) and the critical

angle of inclination of the crack, a key parameter in beam-column joint shear and axial capacity. The figure suggests an inverse proportionality reflected by a power based relationship that can be fitted directly relating drift ratio and normalized axial load as:

$$\left(\frac{\Delta}{L}\right)_{axial} = 0.057 \left(\frac{P \cdot \tan \theta}{A_{sb} f_{yb}}\right)^{-0.5} \quad (24)$$

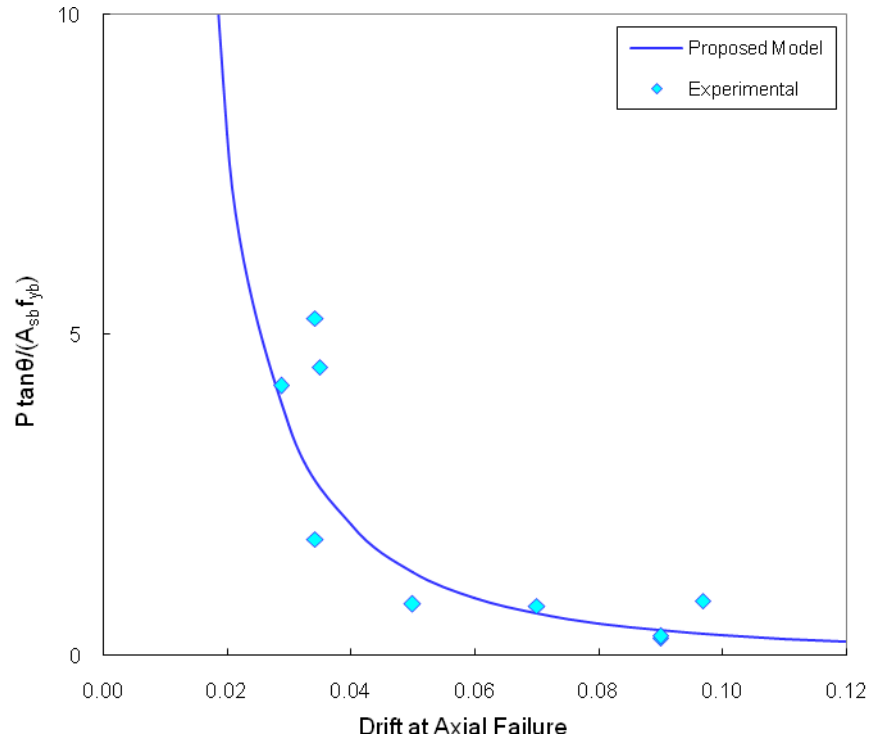


**Fig. 9 – Proposed Empirical Model (Eq. 25) for Drift Capacity at Axial Failure**

It was worthy also investigating the influence of other important parameters such as the concrete strength, joint effective area and column longitudinal reinforcement strength. These factors are common in axial capacity studies of columns. The results of this investigation presented in Hassan (2011) suggested weak sensitivity of the axial failure model to these parameters.

The above discussion suggests the appropriateness of the empirical expression (Eq. 24) for quick estimation of drift capacity at joint axial failure. It is important to notice that this expression is based on a rather small joint axial failure database. Thus, more joint axial failure tests are needed to further verify this relation. In addition, it is worth mentioning that this expression is suitable for J-Failure joints with any axial load ratio, BJ-Failure joints with small axial load ratio, and BJ-Failure with high axial load ratio when the flexural capacity of the beam is close to the direct J-Failure strut-and-tie model capacity. The case of high axial load on a joint in a subassembly where the beam flexural capacity is much smaller than the direct J-failure capacity is excluded from the application of this model.

#### 4.4. Axial Capacity Models Evaluation

Figure 10 presents the correlation of the experimental drift capacity at axial failure to the calculated one using the shear-friction model for axial capacity (Eq. 19). The average test to model drift ratio is 1.00 and the COV is 0.27. It is also worth mentioning that residual shear capacity at axial failure is based on the NEES joint results; which led to the drift for other tests loaded with greater number of displacement cycles

to be overestimated by the model. The empirical axial capacity model proposed by Eq. 24 is also evaluated against test results in Fig. 10. The mean ratio of test-to-model drift capacity was 1.07 and COV of 0.26.

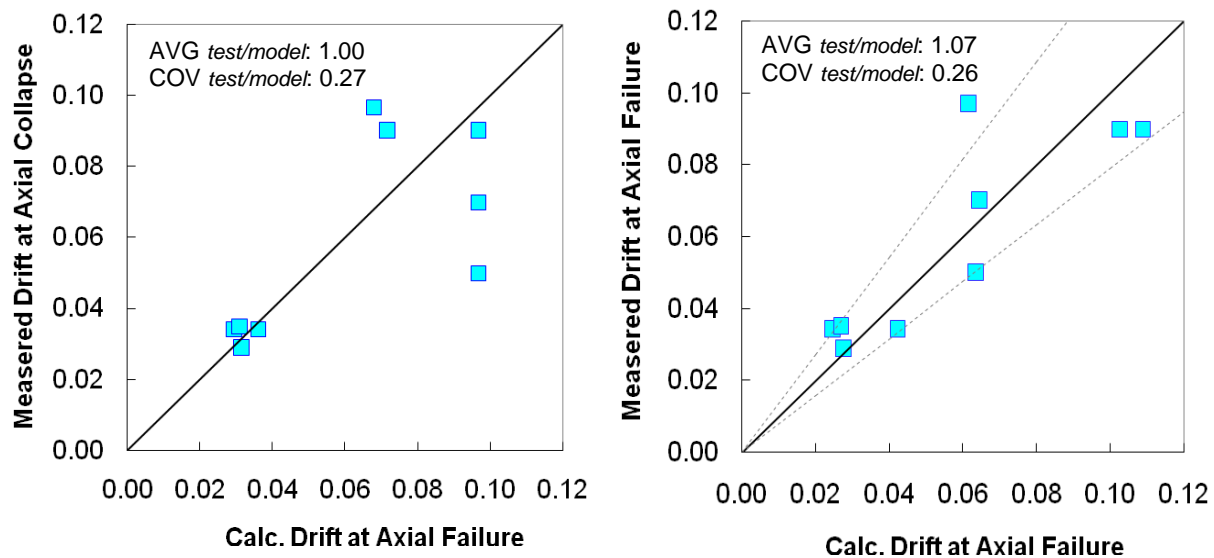


**Fig. 10 – Correlation of the Proposed Axial Capacity Models to Test Results**

## 5. Conclusions

An analytical study was conducted aiming to develop mathematical tools for practical seismic strength assessment of exterior and corner beam-column joints without transverse reinforcement. Within the scope of the parameters and databases considered, the following conclusions can be drawn:

1. A strut-and-tie model for J-Failure unconfined joint shear strength calculation was proposed. This model is based on the ACI 318-11 strut-and-tie modeling provisions interpreted and modified to suite beam-column joints. Effects of axial load level, joint aspect ratio, and bidirectional loading were included in this model. The model correlates well with test results for unconfined exterior and corner beam-column joints.
2. An empirical model for quick estimation of shear strength of unconfined exterior and corner joint with J-Failure mode was proposed. The model accounts for axial load level, joint aspect ratio, and bidirectional loading. The model can estimate joint shear strength for preliminary analysis with reasonable accuracy.
3. An empirical model for estimation of pull-out capacity of insufficiently embedded reinforcement in beam-column joints was proposed. The model accounts for axial load level, transverse beam confinement, and concrete slab effect. The model correlates to test results with reasonable accuracy.
4. The main resisting mechanism that supports axial loads in a shear damaged joints is believed to be shear friction on the previously damaged shear failure plane. The buckling capacity of column reinforcement is believed to be a secondary mechanism to shear friction mechanism, which is triggered upon shear friction failure.
5. An “axial failure safe zone” was identified based on previous tests with and without axial failure. Joint axial failure was not observed for drift ratio demand below 2.5% - 3%. For drift ratios higher than 2.5% - 3%, axial failure was observed especially with increasing drift, axial load, or both.
6. Joint axial capacity models were proposed based on the shear friction concept. The models correlated relatively well with available data, but the data set was relatively small, such that additional model calibration is warranted.

## 6. Acknowledgements

Financial assistance provided by U.S. National Science Foundation (NSF) award #0618804 through George E. Brown Jr. Network for Earthquake Engineering Simulation (NEES) and the Egyptian Department of Higher Education award #2005292 through Building National Research Center is greatly appreciated.

## 7. References

- ELWOOD, K. J., and MOEHLE, J. P., "Shake Table Tests and Analytical Studies on the Gravity Load Collapse of Reinforced Concrete Frames". *PEER Report 2003-01, Pacific Earthquake Engineering Research Center (PEER)*, University of California, Berkeley, 2003.
- HASSAN, W. M., "Analytical and Experimental Investigation of Seismic Vulnerability of Beam-Column Joints without Transverse Reinforcement in Concrete Buildings", *PhD Dissertation, University of California, Berkeley*, May 2011.
- HASSAN, W. M. and MOEHLE, J. P., "Experimental Assessment of Seismic Vulnerability of Corner Beam-Column Joints in Older Concrete Buildings", *Proceedings of the 15<sup>th</sup> World Conference of Earthquake Engineering*, Lisbon, Portugal, September, 2012.
- HASSAN, W. M. and MOEHLE, J. P., "Quantification of Residual Axial Capacity of Beam-Column Joints in Existing Concrete Buildings under Seismic Load Reversals", *Proceedings of the 4<sup>th</sup> International Conference on Computational Methods in Structural Dynamics and Earthquake Engineering*, M. Papadrakakis, V. Papadopoulos, V. Plevris (eds.), Kos Island, Greece, 12- 14 June, 2013.